Design of binary diffractive microlenses with subwavelength structures using the genetic algorithm

Tatsuya Shirakawa,[1] Kenichi L. Ishikawa,[1,2,*] Shuichi Suzuki, [3] Yasufumi Yamada, [3] and Hiroyuki Takahashi[1]

[1]*Department of Nuclear Engineering and Management, School of Engineering, The University of Tokyo, 7-3-1 Hongo, Bunkyo-ku, Tokyo, Japan*
[2]*Photon Science Center, School of Engineering, The University of Tokyo, 7-3-1 Hongo, Bunkyo-ku, Tokyo, Japan*
[3]*RICOH COMPANY, Ltd., Corporate Technology Development Group, 16-1 Shinei-cho, Tsuzuki-ku, Yokohama, Japan*
**ishiken@atto.t.u-tokyo.ac.jp*

Abstract: We present a method to design binary diffractive microlenses with subwavelength structures, based on the finite-difference time-domain method and the genetic algorithm, also accounting for limitations on feature size and aspect ratio imposed by fabrication. The focusing efficiency of the microlens designed by this method is close to that of the convex lens and much higher than that of the binary Fresnel lens designed by a previous method. Although the optimized structure appears to be a binary Fresnel lens qualitatively, it is hard to quantitatively derive directly from the convex Fresnel lens. The design of a microlens with reduced chromatic aberration is also presented.

OCIS codes: (050.6624) Subwavelength structures; (050.1965) Diffractive lenses; (260.2110) Electromagnetic optics.

References and links

1. V. A. Soifer, *Methods for Computer Design of Diffractive Optical Elements (Wiley Series in Lasers and Applications)* (John Wiley & Sons, 2002).
2. D. C. O'Shea, T. J. Suleski, A. D. Kathman, and D. W. Prather, *Diffractive Optics: Design, Fabrication, and Test* (SPIE, 2003).
3. H. Kikuta, H. Toyota, and W. Yu, "Optical Elements with Subwavelength Structured Surfaces," Opt. Rev. **10**(2), 63–73 (2003).
4. G. Saavedra, W. D. Furlan, and J. A. Monsoriu, "Fractal zone plates," Opt. Lett. **28**(12), 971–973 (2003).
5. Y. Okuno, M. Fujimoto, and T. Matsuda, "Numerical evaluation of diffractive optical elements with binary subwavelength structures," IEIC Tech. Rep. **100**, 157–162 (2001) (Japanese).
6. J. N. Mait, D. W. Prather, and M. S. Mirotznik, "Binary subwavelength diffractive-lens design," Opt. Lett. **23**(17), 1343–1345 (1998).
7. D. W. Prather, J. N. Mait, M. S. Mirotznik, and J. P. Collins, "Vector-Based synthesis of finite aperiodic subwavelength diffractive optical elements," J. Opt. Soc. Am. A **15**(6), 1599–1607 (1998).
8. D. A. Pommet, M. G. Moharam, and E. B. Grann, "Limits of scalar diffraction theory for diffractive phase elements," J. Opt. Soc. Am. A **11**(6), 1827–1834 (1994).
9. A. Taflove, "Application of the finite-difference time-domain method to sinusoidal steady-state electromagnetic-penetration problems," IEEE Trans **22**, 191–202 (1980).
10. M. G. Moharam, E. B. Grann, D. A. Pommet, and T. K. Gaylord, "Formulation for stable and efficient implementation of the rigorous coupled-wave analysis of binary gratings," J. Opt. Soc. Am. A **12**(5), 1068–1076 (1995).
11. S. Kirkpatrick, C. D. Gelatt, Jr., and M. P. Vecchi, "Optimization by Simulated Annealing," Science **220**(4598), 671–680 (1983).
12. M. Mitchell, *An Introduction to Genetic Algorithms* (MIT Press, 1998).
13. E. G. Johnson, and M. A. G. Abushagur, "Microgenetic-algorithm optimization methods applied to dielectric gratings," J. Opt. Soc. Am. A **12**(5), 1152–1160 (1995).
14. C. F. Huang, and H. M. Li, ""Design optimization of chip antennas using the GA-FDTD approach", Int. J. RF Microw," Computer-Aided Engineering **15**, 116–127 (2005).
15. H. Jimbow, C. Yatabe, K. L. Ishikawa, Y. Yamada, and K. Masuda, "Design of subwavelength diffractive optical elements using genetic algorithm and FDTD method," IEEJ Trans. EIS **127**(9), 1298–1303 (2007) (Japanese).

#124061 - $15.00 USD Received 9 Feb 2010; revised 4 Apr 2010; accepted 5 Apr 2010; published 6 Apr 2010

16. A. Taflove, and S. C. Hagness, *Computional Electrodynamics: The Finite-Difference Time-Domain Method*, Chap. 12 (Artech House, 2005).
17. J. P. Berenger, "A perfectly matched layer for the absorption of electro-magnetic waves," J. Comput. Phys. **114**(2), 185–200 (1994).
18. K. Ono, and K. Eriguchi, "Modeling of plasma-surface interactions and profile evolution during dry etching," J. Plasma Fusion Res. **85**, 165–176 (2009) (Japanese).

1. Introduction

Diffractive optical elements (DOEs) control propagations and characteristics of the lightwave by diffractions of the continuous relief structure of the surface [1,2], and can be used for precision laser beam control and shaping. Recent advances in the microfabrication technology enable to fabricate DOEs with structures finer than the optical wavelength, namely, subwavelength structures (SWSs) [3].

In this study, we consider the design of binary diffractive microlenses with SWSs. Although zone plates with a fractal structure [4] have also been reported, most of the previous methods [5–7] use the Fresnel lens as a starting point and rely on the scalar diffraction theory. However, in general, the scalar diffraction theory leads to a significant error when the feature size is less than 14 wavelengths [8], and cannot be applied when the latter is smaller than the wavelength. Therefore, it is desirable to rigorously analyze the behavior of the light by solving the Maxwell's equations with the finite-difference time-domain (FDTD) method [9] or the rigorous coupled-wave analysis [10]. However, in its turn, this imposes another problem: the behavior of the electromagnetic wave in SWSs is so complex that there is no simple design strategy. To overcome this difficulty, for the case of periodic gratings, the optimization by the simulated annealing [11] and the genetic algorithm (GA) [12] has been proposed [13]. We have also recently developed a method based on the combination of the FDTD and GA (GA-FDTD method [14]) and successfully designed polarization beam splitters [15].

Here, we extend the GA-FDTD method to design a subwavelength-structure aperiodic diffractive optical elements, in particular, binary diffractive microlenses. The designed lens has focusing efficiency much higher than the binary lens designed by a previous method [5] and close to that of the convex lens. The precise features of the obtained structure, which qualitatively appears to be a binary Fresnel lens, cannot be expressed as a simple binarization of the convex Fresnel lens. We also successfully design a binary lens with reduced chromatic aberration. The obtained structure is even harder to deduce intuitively. This indicates the effectiveness of our method for designing subwavelength-structure diffractive optical elements.

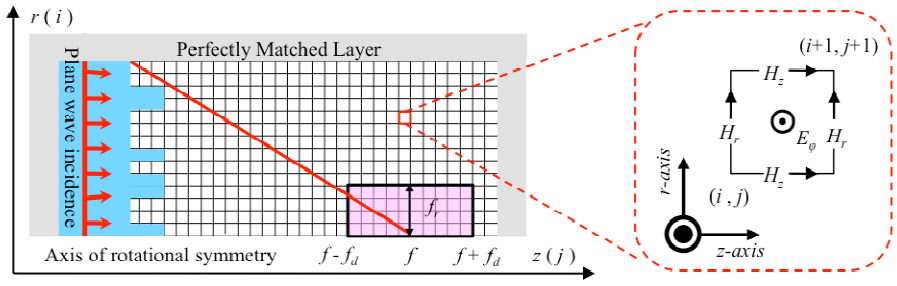

Fig. 1. Schematic of the analytical domain rotationally symmetric about the z-axis. A plane wave is incident from the left to the microlens (blue region). The close-up on the right indicates the electromagnetic components on the BOD-FDTD calculation grid. (i, j) are indexes for the spatial coordinate (i and j for the radial and z directions, respectively).

#124061 - $15.00 USD Received 9 Feb 2010; revised 4 Apr 2010; accepted 5 Apr 2010; published 6 Apr 2010

2. Computational approach

2.1 Bodies of revolution (BOR) FDTD method

We apply the BOR-FDTD method [16] to electromagnetic calculations for a system of axial symmetry. The perfectly matched layer absorbing boundary condition [17] is used. The domain we consider is rotationally symmetric about the z-axis, and the propagation direction of the incident plane wave is parallel to the axis (Fig. 1).

2.2 Genetic Algorithm (GA)

We optimize the structure of the binary diffractive microlens (blue region in Fig. 1) using the genetic algorithm (GA) [12]. GA is an optimization method that uses techniques inspired by evolutionary biology such as the inheritance, mutation, selection, and crossover. We first encode the relief pattern (grating alignment) and grating height (phenotype or PTYPE) in a binary string (genotype or GTYPE). Two kinds of coding are used as follows. IIIn consideration of actual fabrication possibility, we impose conditions that the grating width is 100 nm at least, and the aspect ratio is 5 at most.

Coding #1 (Fig. 2): The first 200 bits express the binary relief pattern in the r direction. One bit corresponds to a width Δd of 20 nm and the lens radius is 4 μm. Then, the grating height is coded by 4 bits from 200 to 500 nm with a step of 20 nm. An advantage of this coding is that it is simple and general, requires no prior knowledge, and, thus, can also be applied to different kinds of DOEs.

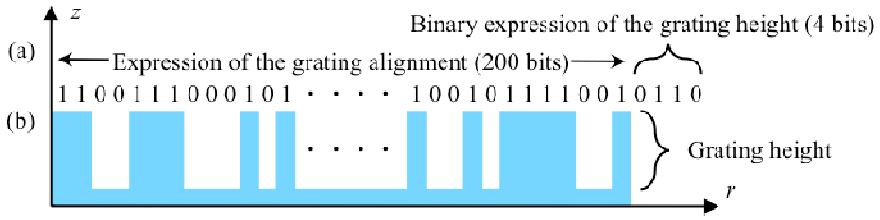

Fig. 2. Mapping between (a) Genotype and (b) Phenotype in Coding #1.

Coding #2 (Fig. 3): After some trials, we notice that phenotypes of better performance are composed of inner and outer parts separated by a space in general, as we will see later in Sec. 3. Thus, let us reflect this in the coding by assigning additional 7 and 5 bits to the width of the inner part and the space, respectively. Then those of the first 200 bits that correspond to the space are disregarded when mapped to the phenotype. While this coding is inspired a posteriori by the feature observed during the optimization using Coding #1, it should be noted that any arbitrary phenotype expressed by Coding #1 can also be expressed by Coding #2, since the space width can be zero. Thus, the solution space is not reduced by the introduction of Coding #2 and as general as for #1.

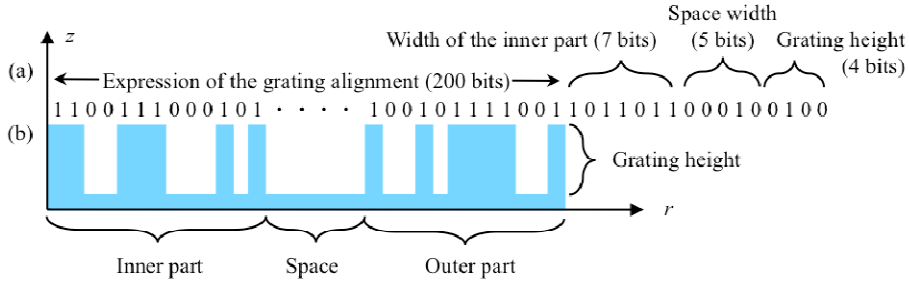

Fig. 3. Mapping between (a) Genotype and (b) Phenotype in Coding #2.

We evaluate the fitness F of each genotype using the focusing performance as,

#124061 - $15.00 USD Received 9 Feb 2010; revised 4 Apr 2010; accepted 5 Apr 2010; published 6 Apr 2010

$$F = \frac{\left(f_d - \left|f_o - f\right|\right)}{f_d} \times \sum_{z=f-f_d}^{f+f_d} \sum_{r=0}^{f_r} S_z(r,z), \quad (1)$$

where S_z denotes the z-component of the Poynting vector (intensity), f_0 and f the targeted and actual focal distance, respectively, and f_d and f_r the length and radius, respectively, of the evaluation domain (shown in Fig. 1). The stronger the focusing around the targeted focal point, the higher the fitness value takes.

Based on the value of the fitness function, the parents for the next generation are selected by the roulette-wheel selection and the elite strategy. The children are produced through the process of the uniform crossover and the invert mutation.

2.3 GA-FDTD method

The design procedure using the GA is summarized as follows.

(1) Randomly prepare sixteen GTYPEs as the initial generation.

(2) Evaluate the fitness of each GTYPE belonging to the generation, by FDTD calculation for the corresponding PTYPE.

(3) Select eight pairs of GTYPEs according to their fitness by the roulette-wheel selection

(4) Apply the uniform crossover (crossover rate: 0.95) and mutation (mutation rate: 0.01) to create new GTYPEs, which form the next generation

(5) Then start again from (2)

We made a preliminary survey on the sensitivity of the results to the GA parameters (group size M, crossover rate P_c, and mutation rate P_m) by comparing the fitness values after 1000 generations with Coding #1. We first varied P_m between 0.005 and 0.2, while fixing M = 16, and P_c = 0.3 and 0.9. For both values of P_c the fitness value was highest at P_m = 0.01. Next, by fixing M = 16 and P_m = 0.005 and 0.01, we varied P_c between 0.1 and 1, and found that the fitness value was generally high for P_c = 0.9 - 1. Finally, we varied M between 8 and 40. The obtained fitness value was low at M = 8 but approximately equally high between M = 16 and 40. Based on these observations, we have chosen, as GA parameter values, M = 16, P_c = 0.95, and P_m = 0.01 to obtain the results presented in what follows. We have also confirmed that all the tested parameter combinations yield similar structures in the end.

By far the most time-consuming part, i.e., FDTD calculation can be done independently for each GTYPE. Thus, the GA procedure can be efficiently parallelized. We perform GA-FDTD optimization using eight processing-elements (cores) on a single workstation equipped with two quad-core Intel Xeon processors. The typical computational time is approximately three minutes per generation.

While most of the results presented in this paper are obtained with Coding #1, the performance of the two is compared in Subsec. 3.4.

3. Results

3.1 Optimally-designed microlens and its focusing performance

In this study we set the lens radius and targeted focal distance as 4 μm and 8.3 μm (z = 9.3 μm) for 660 nm wavelength, respectively. The refractive index of the material (Ta_2O_5) is assumed to be 2.1466 at this wavelength. The grid size in BOR-FDTD calculations is 20 nm, unless otherwise stated. Figure 4 displays the obtained structure and the intensity distribution of the beam incident from the bottom of the structure as a plane wave. We define the focal distance from the bottom (z = 1 μm) of the gratings. The actual focal distance of the obtained structure is 8.3 μm as targeted. The red curve of Fig. 6(a) shows the intensity distribution in the focal face. The spot radius given by the half width at half maximum (HWHM) is 0.40 μm, and the spot shape is almost circular [Fig. 6(b)]. The focusing efficiency of the obtained

#124061 - $15.00 USD Received 9 Feb 2010; revised 4 Apr 2010; accepted 5 Apr 2010; published 6 Apr 2010

structure, defined as the ratio of the beam power at $r < 1$ μm to the incident power, is 59.3%. Figure 6(a) also compares the results obtained with two different values of grid size (the red curve for 5 nm and the black dashed curve for 20 nm) for FDTD calculations. The difference between the two curves turns out to be less than 0.1%. This result indicates that the FDTD calculation with a grid size of 20 nm is sufficiently accurate.

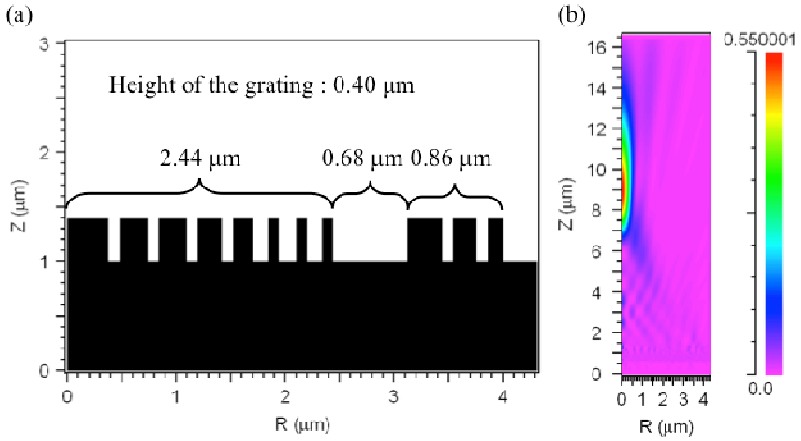

Fig. 4. (a) Structure obtained by the GA-FDTD method (b) Intensity distribution

At first glance, qualitatively, the structure might appear to be a binarization of the convex Fresnel lens with the same focal length. However, quantitatively, this is not the case, as we will see in Subsec. 3.2. Especially, the grating height (400 nm) is different from that of the Fresnel lens (576 nm).

3.2 Comparison with the convex lens, the convex Fresnel lens, and the binary Fresnel lens

Let us compare the focusing performance of the GA-designed structure (Fig. 4) with that of the convex lens, the convex Fresnel lens, and the binary Fresnel lens of the same radius and focal length. The structures and beam intensity distribution of the latter three are displayed in Fig. 5. The binary Fresnel lens is designed by a previously reported procedure [5] based on the scalar diffraction theory reported previously.

Figure 6(a) compares the intensity distribution in the focal face (z = 9.3 μm) for the four lenses. The focusing efficiency of each structure is 59.3%, 79.1%, 70.4%, and 28.0%, respectively. It is remarkable that the performance of the binary microlens designed in this study is more than twice as high as that of the binarization of the Fresnel lens reported previously, and is close to that of the lenses with a curved surface. Moreover, the relation between the widths of neighboring gratings cannot be expressed in a simple way.

From the comparison between Figs. 4 and 5(c), we may notice that the GA-obtained structure is qualitatively similar to the binary Fresnel lens. Especially, both appear to be composed of two parts separated by a space. We have confirmed this trend also for lenses of larger radii; for example, the optimally-designed microlens with a 10 μm radius has three spaces or regions of small grating density (not shown). However, quantitatively, the GA-obtained structure and the binary Fresnel lens are clearly different from each other, and the precise transformation formula from Fig. 5(b) to Fig. 4 is hardly obtainable.

3.3 Effect of fabrication error (trapezoidal gratings)

It has been reported that gratings fabricated with the plasma etching technique may have edge defects [18]. To examine the impact of such a fabrication error, let us model the edge defects by trapezoidal gratings with a base angle of 84.3° (Fig. 7).

As can be deduced from the beam intensity distribution shown in Fig. 7(b), the focusing efficiency of the microlens with the mimicked edge defects (63.7%) is even slightly higher

#124061 - $15.00 USD Received 9 Feb 2010; revised 4 Apr 2010; accepted 5 Apr 2010; published 6 Apr 2010

than that of the defect-free structure (59.3%). This result indicates that the GA-designed binary structure is robust against this type of fabrication error.

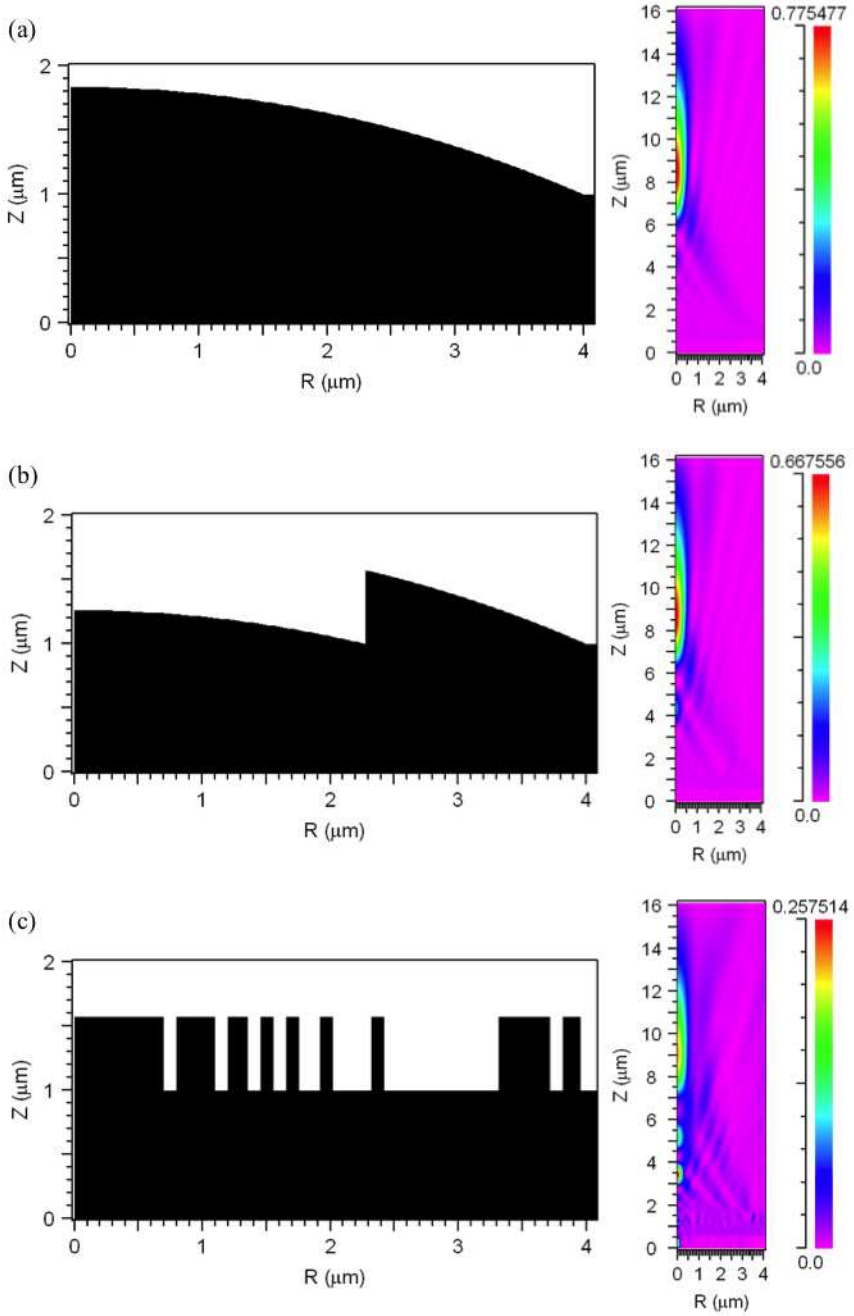

Fig. 5. (a) The convex lens and (b) its Fresnel lens and (c) binarization of the Fresnel lens [5]

#124061 - $15.00 USD Received 9 Feb 2010; revised 4 Apr 2010; accepted 5 Apr 2010; published 6 Apr 2010

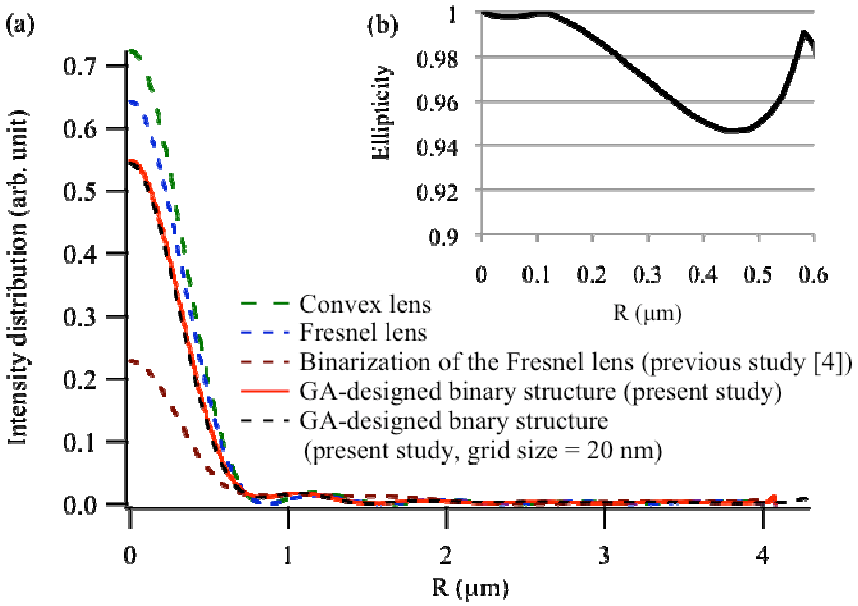

Fig. 6. (a) Focusing performance comparison of the GA-designed structure with the convex lens, its Fresnel lens, and binarization of the Fresnel lens in focal face (Z = 9.3 μm). The grid size used in FDTD calculations is 5 nm except for the black dashed curve. (b) Ellipticity of the spot shape.

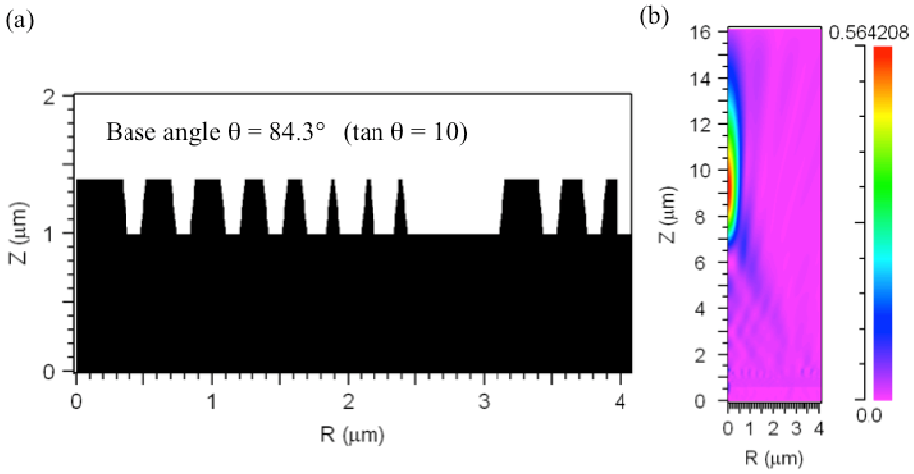

Fig. 7. (a) Trapezoidal gratings based on the GA-designed structure (b) intensity distribution

3.4 Comparison of the coding methods

Figure 8 compares the history of the fitness evolution for the two different coding methods in Subsec. 2.2. The fitness increases significantly faster with Coding #2 than with #1. Hence, by making use of information and guiding principle, even qualitative, found in the early states of optimization, we can significantly accelerate the convergence to the optimum solution.

#124061 - $15.00 USD Received 9 Feb 2010; revised 4 Apr 2010; accepted 5 Apr 2010; published 6 Apr 2010

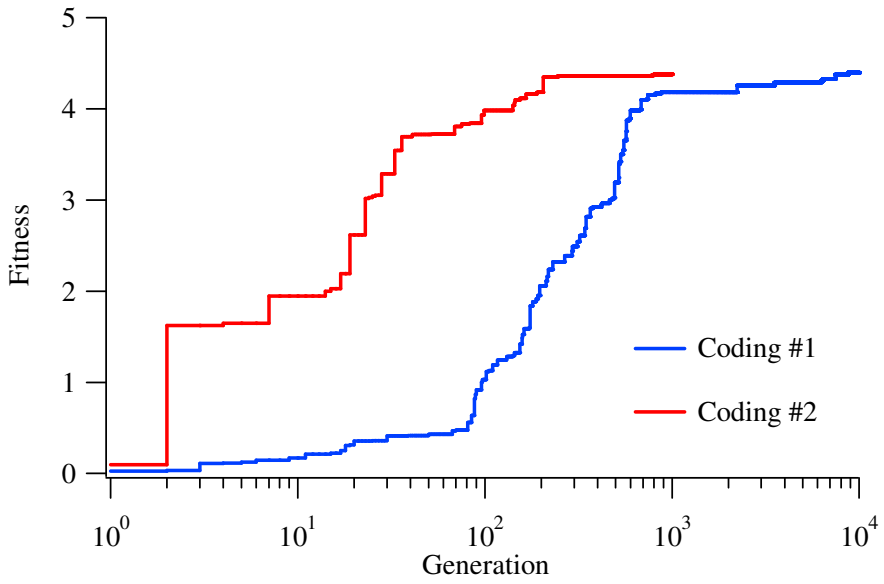

Fig. 8. Evolution of the fitness as a function of generation for two differenct coding methods.

3.5 Design of a binary lens with reduced chromatic aberration at three wavelengths

As another example, let us now apply the GA-FDTD method to the design of a binary microlens that has similar focal lengths at three wavelengths of 660 nm, 532 nm, and 445 nm. Refractive indexes of the material are 2.1919 and 2.2577 at 532 nm and 445 nm, respectively. Figure 9 shows the structure obtained with coding #2 and the intensity distribution of the beams of the three wavelengths. Again, the grating alignment is not intuitive, and would be even harder to deduce from experience and a simple theory than that of the monochromatic microlens (Fig. 4).

Figure 10 displays the focal distance and efficiency of the designed lens as a function of the wavelength. It should be noted that the structure in Fig. 4 does not function as a lens below 470 nm. We can clearly see that the chromatic aberration is much reduced and the focusing efficiency is flattened compared with that of the structure in Fig. 4. Its focusing efficiency is 38.0%, 32.4%, and 30.6% at 660 nm, 532 nm, and 445 nm, respectively. Although these values are lower than for the case of the GA-optimized monochromatic lens (Fig. 4), they are still higher than that of the binary Fresnel lens of Fig. 5(c).

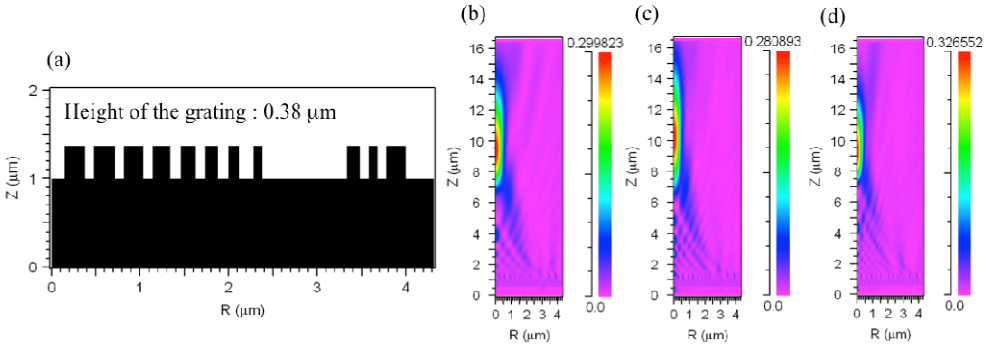

Fig. 9. (a) Binary lens with reduced chromatic aberration at three wavelengths designed by the GA-FDTD method and intensity distributions for plane wave incidence with a wavelength of (b) 660 nm, (c) 532nm, (d) 445 nm

#124061 - $15.00 USD Received 9 Feb 2010; revised 4 Apr 2010; accepted 5 Apr 2010; published 6 Apr 2010

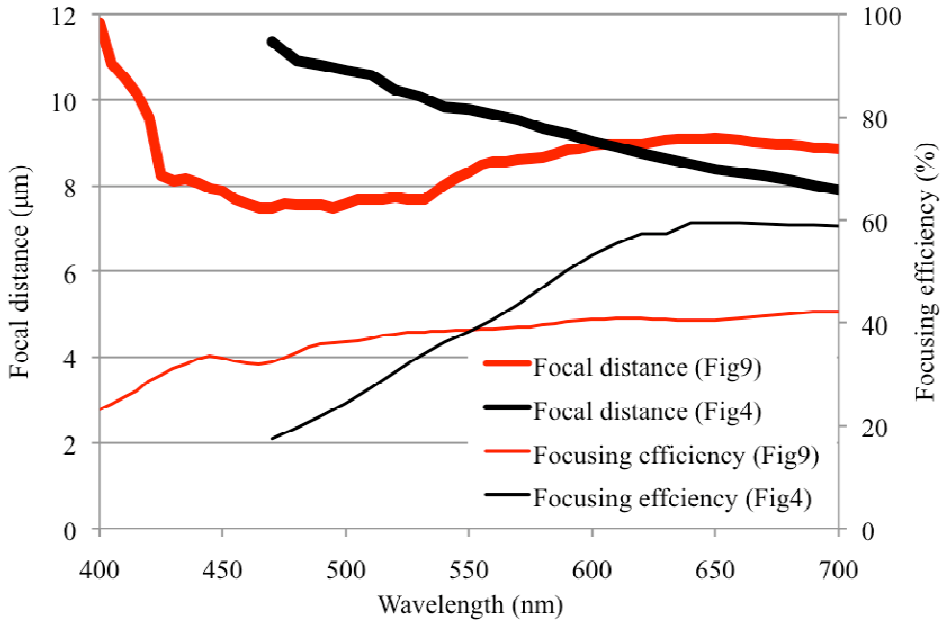

Fig. 10. Focal distance (left axis) and efficiency (right axis) of two different microlenses (Figs. 4 and 9). The structure depicted in Fig. 4 does not work as a lens below 470 nm.

4. Conclusion

We have presented a procedure for the design of binary diffractive microlenses with subwavelength structures, based on the combination of the exact electromagnetic calculation with the FDTD method and the optimization through the genetic algorithm. The procedure can be easily applied to different kinds of periodic and aperiodic diffractive optical elements. The microlens we have designed has focusing performance is significantly higher than that of the binary Fresnel lens designed with the previous method [5] and even close to that of the convex Fresnel lens. We have also successfully designed a microlens with reduced chromatic aberration. Although the obtained structures are qualitatively similar to that of the binary Fresnel lens, their precise quantitative features appear to be hard to derive through other simple theoretical insights. This indicates that the GA-FDTD method is effective in the design of diffractive optical elements with subwavelength features, in which the electromagnetic field exhibits complex behavior.

Acknowledgment

This work has been partially supported by the Advanced Photon Science Alliance (APSA) project (Japan).

#124061 - $15.00 USD Received 9 Feb 2010; revised 4 Apr 2010; accepted 5 Apr 2010; published 6 Apr 2010